

Finite element method application of ERBS triangles

Tatiana Kravetc

R&D group Simulations

Department of Computer Science and Computational Engineering

Faculty of Science and Technology

UiT – The Arctic University of Norway

Abstract

In this paper we solve an eigenvalue problem on a circular membrane with fixed outer boundary by using a finite element method, where an element is represented as an expo-rational blending triangle.

ERBS triangles combine properties of B-spline finite elements and standard polynomial triangular elements. The overlapping of local triangles allows us to provide a flexible handling of the surface while preserving the smoothness of the initial domain, also over the nodes and edges. Blending splines accurately approximate the outer boundary, while keeping a coarse discretization of the domain.

We consider a mesh construction for such type of elements, evaluating of basis functions and their directional derivatives, local-to-global mapping, assembling of element matrices.

1 Introduction

Isogeometric analysis invokes a methodology that represents the solution space for dependent variables in terms of the same functions which represent the geometry [1].

Triangulation is a common approach to the domain discretization. Triangulation is more general than the tensor product surfaces, due to less geometrical constraints. When approximating solutions by the finite element method, we should choose the finite element mesh in such a way that it must not only get an accurate approximate solution but also the edges of the outer elements must approximate the boundary well. Triangular elements are particularly suited to the task of filling domains with smooth boundaries, thus minimizing the difference between the initial domain and the finite element domain [2].

One way to increase the accuracy of the solution is to provide mesh refinement, i.e. increase the number of elements, especially along the smooth boundary. Another way is to refine the elements. It implies higher-degree polynomials in the basis functions, and a mapping between local and global coordinate systems.

In this paper we introduce ERBS triangles as an alternative type of elements. These elements are based on expo-rational blending splines, which have been introduced in [3]. ERBS triangles are defined in [4]. The main distinction between B-splines and expo-rational blending surfaces is that the second ones can be relatively easy evaluated on a triangular mesh. The reason for this is that the expo-rational basis possesses an interpolatory property and it is strictly local under the support of the local geometry. In the presented research we show that the mesh constructed by ERBS triangles gives a very good approximation of the PDE solution with very coarse domain discretization, but geometrically exact at the boundary.

The following related works demonstrate an utilization of blending spline surfaces on triangulations. An implementation of the spline blending surface approximation over a triangulated irregular network is shown in [5]. The first instances of expo-rational finite elements on triangulations was presented in [6] and their application can be found in [7].

This paper is organized as follows: Section 2 focuses on basis functions, which combine ERBS basis and Bernstein polynomial basis of local triangles. In Section 3 we define a model problem and derive the finite element method applied to the considered problem, utilizing the ERBS triangles as elements. In Section 4 we show the results of the described method, implemented in MatLab, and compare them to the exact solution. The conclusions are given in Section 5.

2 ERBS triangles

In this section we collect previous results from [3], [4] and consider a construction of ERBS triangles, a combination of barycentric representation of Bernstein basis polynomials and expo-rational basis, and its directional derivatives.

An ERBS triangle is a surface that blends three Bézier triangles of the degree d via expo-rational basis functions. A comprehensive study of barycentric coordinates and Bézier triangles can be found in [8]. We define a simple version of the underlying basic expo-rational basis function over the formal parameter u .

Definition 2.1. The underlying basic expo-rational basis function in barycentric coordinates is defined by $B(u)$, $u \in (0, 1]$, as follows

$$B(u) = \begin{cases} \Gamma \int_0^u \phi(s) ds, & \text{if } 0 < u \leq 1, \\ 0, & \text{otherwise} \end{cases}$$

where

$$\phi(u) = \exp \left(- \frac{\left(u - \frac{1}{2} \right)^2}{u(1-u)} \right),$$

and the scaling factor

$$\Gamma = \frac{1}{\int_0^1 \phi(u) du}.$$

A set of such expo-rational functions forms a basis for the blending type surface construction.

Definition 2.2. For any point $\nu = (u_1, u_2, u_3)$, $u_1 + u_2 + u_3 = 1$, a set of expo-rational basis functions in barycentric coordinates is defined as follows

$$\beta_i(\nu) = \frac{B(u_i)}{B(u_1) + B(u_2) + B(u_3)} \quad \text{for } i = 1, 2, 3, \quad (1)$$

where $B(u_i)$ are as defined by Definition 2.1.

A set of expo-rational basis functions on a triangle is shown in Figure 1(a).

A construction of an ERBS triangle is based on a linear combination of three Bézier triangles of degree d and the set of expo-rational basis functions in barycentric coordinates.

Definition 2.3. For a set of local Bézier triangles $\ell_i(u_1, u_2, u_3)$, $i = 1, 2, 3$, and corresponding expo-rational basis functions $\beta_i(u_1, u_2, u_3)$, the general formula for the ERBS triangle is

$$S(u_1, u_2, u_3) = \sum_{i=1}^3 \ell_i(u_1, u_2, u_3) \beta_i(u_1, u_2, u_3), \quad (2)$$

where $u_1 + u_2 + u_3 = 1$ and $u_1, u_2, u_3 \geq 0$.

So far we have collected results from previous work on ERBS on triangular domains.

To use the ERBS triangles in a finite element context, we need to introduce a basis for ERBS triangle that combines both Bernstein basis and expo-rational basis. Locally, i.e. on the one ERBS triangle, the number of combined basis functions is equal to $q = 3 \binom{d+2}{2}$.

The Bernstein polynomial basis, defined on the triangle K , can be written as a matrix W with ordered elements

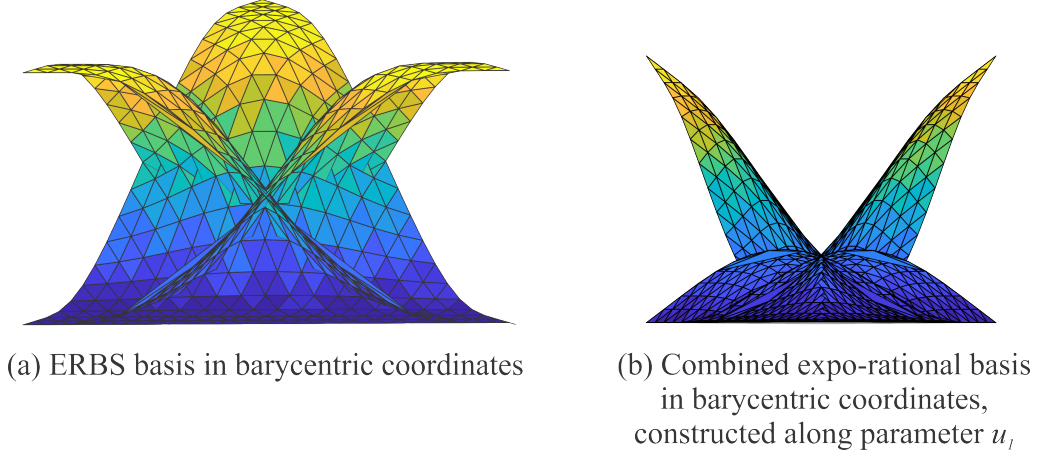


Figure 1: Basis functions in barycentric coordinates.

$$W_d^K = [b_{0,0,d}^d \quad b_{0,1,d-1}^d \quad \dots \quad b_{d,0,0}^d],$$

where

$$b_{i,j,k}^d = \frac{d!}{i!j!k!} u^i v^j w^k, \quad u + v + w = 1.$$

Then the combined basis $G^K = G^K(u_1, u_2, u_3)$ on the same triangle is formulated as

$$G^K = [\beta_1 W_d^K \quad \beta_2 W_d^K \quad \beta_3 W_d^K]. \quad (3)$$

Thus, the formula (2) can be rewritten in a compact matrix form as

$$S(u_1, u_2, u_3) = (P^K)^T G^K, \quad (4)$$

where P^K is a set of corresponding coefficients of three local triangles.

Figure 1(b) demonstrates a set of combined expo-rational basis functions G^K , evaluated along one of parameters, the degree of local triangles is equal to 1.

Figure 2 shows an example of ERBS triangle with local Bézier triangles of degree 1. This construction is very flexible and can be fitted to a geometry of relatively high degree of smoothness.

We now construct a set of partial derivatives of the combined expo-rational basis.

Definition 2.4. Let $D_{u_\iota} W_d^K$ be a set of directional derivatives in the direction u_ι of Bernstein basis functions of degree d . Then, from (3), it follows that the partial derivatives of the combined expo-rational basis in barycentric coordinates can be found as

$$D_{u_\iota} G^K = \begin{bmatrix} D_{u_\iota} \beta_1 W_d^K + \beta_1 D_{u_\iota} W_d^K \\ D_{u_\iota} \beta_2 W_d^K + \beta_2 D_{u_\iota} W_d^K \\ D_{u_\iota} \beta_3 W_d^K + \beta_3 D_{u_\iota} W_d^K \end{bmatrix} = \begin{bmatrix} D_{u_\iota} \beta_1 & \beta_1 \\ D_{u_\iota} \beta_2 & \beta_2 \\ D_{u_\iota} \beta_3 & \beta_3 \end{bmatrix} \begin{bmatrix} W_d^K \\ D_{u_\iota} W_d^K \end{bmatrix},$$

for each $\iota = 1, 2, 3$.

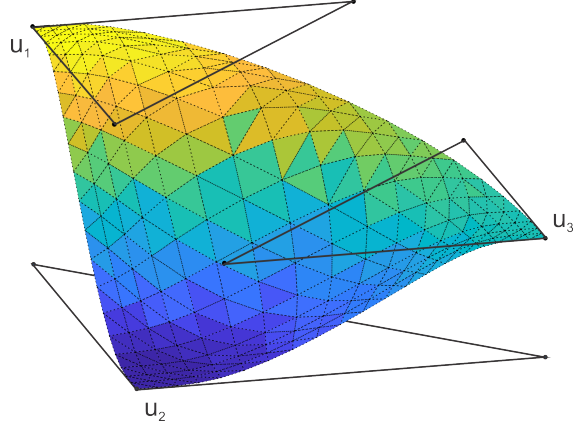


Figure 2: An example of the ERBS triangle with local Bézier triangles of the first degree.

3 Model problem

In this section we demonstrate an exact solution of the eigenvalue problem on a circular membrane and its approximation using the finite element method.

A detailed description of obtaining an analytical solution of the problem of membrane vibrations can be found in [9]. Consider a circular membrane Ω having a radius $r = a$ and a fixed outer boundary $\partial\Omega$. Introduce a given material constant c and a circular frequency ω .

Define the eigenvalue problem in the following form

$$\Delta\vartheta + \frac{\omega^2}{c^2}\vartheta = 0, \quad \text{in } \Omega, \quad (5)$$

$$\vartheta = 0, \quad \text{on } \partial\Omega. \quad (6)$$

An analytical solution of the problem (5) with boundary condition (6) is represented by two independent orthogonal eigenfunctions, referred to as the cosine and the sine modes, respectively

$$\vartheta_C^{(m,n)} = J_m(\omega_{(m,n)}r/c) \cos m\phi \quad \text{and} \quad \vartheta_S^{(m,n)} = J_m(\omega_{(m,n)}r/c) \sin m\phi, \quad (7)$$

where J_m is a Bessel function.

The circular eigenfrequencies $\omega_{(m,n)}$ of the (m, n) mode can be found from the formula

$$\gamma = \omega/c.$$

The eigenvalues $a\gamma_{(m,n)}$ denote from the boundary condition (6), which yields the characteristic equation

$$J_m(\gamma a) = 0.$$

Now, we consider a discrete solution for the eigenvalue problem. A detailed finite element approach is described in [10].

By replacing $\frac{\omega^2}{c^2} = \lambda$, we formulate the finite element method for the problem (5)-(6) as follows

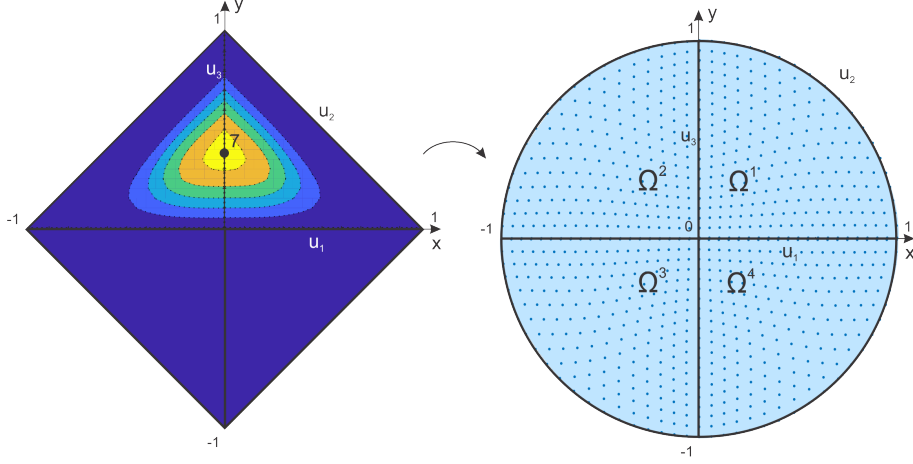


Figure 3: A mapping between triangular mesh and circular domain. A contour plot of seventh combined expo-rational basis function is shown on the left figure. Parameter lines of the circular domain are show on the right figure.

$$\left(\int_{\Omega} \nabla \mathbf{G}^T \nabla \mathbf{G} d\Omega + \int_{\partial\Omega} \kappa \mathbf{G}^T \mathbf{G} d(\partial\Omega) \right) \zeta = \lambda \int_{\Omega} \mathbf{G}^T \mathbf{G} d\Omega \zeta, \quad (8)$$

where \mathbf{G} is a set of all basis functions G^K , defined on the triangulated domain Ω .

In a compact matrix representation (8) is written as

$$(A + R)\zeta = \Lambda M\zeta, \quad (9)$$

where A is the stiffness matrix, M is the mass matrix and R is the boundary matrix.

The eigenvectors ζ and eigenvalues Λ come in pairs (ζ, Λ) , and there are as many pairs $(\zeta_i, \Lambda_i)_{i=1}^n$ as there are coefficients \mathbf{P} . Then the solution ζ_i substitutes the z -coordinate of the coefficients \mathbf{P} and thus the approximation of the eigenfunction ϑ_h can be obtained by the linear combination of coefficients and basis functions.

Domain construction

The main interest of the considered implementation is to explore how the very coarse mesh and low-degree local triangles handle a complex shape of the solution.

A set of combined expo-rational basis functions for one element is defined in Section 2. Each basis function G_i , $i = 1, \dots, n$, is continuous, piecewise, and has its support on a set of corresponding elements.

Let $\mathbf{P} = \{P\}_{i=1}^n$, $P_i \in \mathbb{R}^2$ be a set of coefficients and a set of combined expo-rational basis functions be $\mathbf{G} = \{G_i\}_{i=1}^n$. We divide the entire domain Ω symmetrically into four elements Ω^e , $e = 1, \dots, 4$. One element will be represented as a fixed triangle, with respect to which we will construct an ERBS triangulate surface to approximate a solution of the problem. A set of four elements represents a mesh. A mapping obtained by a linear combination of expo-rational basis functions and local triangles yields an approximation of the real domain. This mapping is shown in Figure 3. The set of coefficients of local triangles is called *a control net*.

A control net based on ERBS triangles has a layered structure in our example. An upper layer consists of four local triangles, which are connected by a central point. A bottom layer consists of triangles, connected by two, which construct the

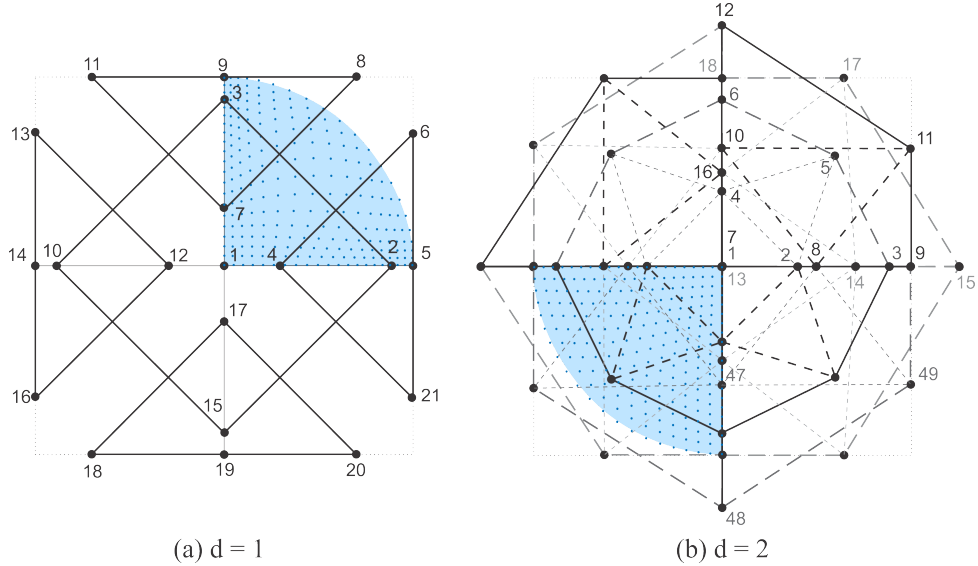


Figure 4: Local triangles and their coefficients of a circular domain, constructed by four ERBS triangles. (a) First degree of local triangles. (b) Second degree of local triangles.

outer boundary. To avoid discontinuity in the domain, we merge together matching points. The number of coefficients n varies depending on the point configuration. A number of basis functions on the entire domain corresponds to the number of control points.

Figure 4 shows two examples of a control net for a mesh, which approximate a circular domain Ω with radius a . Figure 4(a) demonstrates local triangles of degree 1, Figure 4(b) shows local triangles of degree 2. The outer boundary for both cases is approximated by the L^2 -projection and blending splines.

Coordinate transformation

Since the elements that we consider are curvilinear, we need to define coordinate transformations for them to compute the integrals constituting formula (8). Construction of two- and three-dimensional triangular and rectangular isoparametric elements, coordinate transformations and numerical integrations are detailed in [11], and an application of this to a problem of membrane vibration is exploited in [2].

To define correspondence between curvilinear and Cartesian coordinates we first focus on one triangular element Ω^e . The mapping between coordinates was introduced earlier, see formula (4), as a linear combination of control points $P = \{(p_i^x \ p_i^y)\}_{i=1}^q$ and basis functions $G = \{G_i(u_1, u_2, u_3)\}_{i=1}^q$, where $q = 3 \binom{d+2}{2}$. This relation is valid for any local coordinate system. A slight complication with the barycentric coordinates is that they are not independent and the number of them is one more than in Cartesian coordinate system. To avoid this issue, we introduce new dependent formal variables

$$\begin{aligned} \xi &= u_1, \\ \eta &= u_2, \\ 1 - \xi - \eta &= u_3. \end{aligned} \tag{10}$$

For computation of the matrices A , M and R we need to provide two transformations. First, we express global derivatives through local derivatives. Secondly, a differential element of area has to be represented in local coordinates and the integration limits should be correspondingly changed.

We can write partial derivatives with respect to new variables of the basis functions as

$$\begin{aligned}\frac{\partial G_i}{\partial \xi} &= \frac{\partial G_i}{\partial u_1} \frac{\partial u_1}{\partial \xi} + \frac{\partial G_i}{\partial u_2} \frac{\partial u_2}{\partial \xi} + \frac{\partial G_i}{\partial u_3} \frac{\partial u_3}{\partial \xi}, \\ \frac{\partial G_i}{\partial \eta} &= \frac{\partial G_i}{\partial u_1} \frac{\partial u_1}{\partial \eta} + \frac{\partial G_i}{\partial u_2} \frac{\partial u_2}{\partial \eta} + \frac{\partial G_i}{\partial u_3} \frac{\partial u_3}{\partial \eta}.\end{aligned}\quad (11)$$

Using (10) and (11), we get

$$\begin{aligned}\frac{\partial G_i}{\partial \xi} &= \frac{\partial G_i}{\partial u_1} - \frac{\partial G_i}{\partial u_3}, \\ \frac{\partial G_i}{\partial \eta} &= \frac{\partial G_i}{\partial u_2} - \frac{\partial G_i}{\partial u_3}.\end{aligned}\quad (12)$$

Partial derivatives is evaluated by the formula defined in Definition 2.4. At once, the transformation between local coordinates ξ , η and the corresponding global coordinates x , y can be written in matrix form as

$$\begin{bmatrix} \frac{\partial G_i}{\partial \xi} \\ \frac{\partial G_i}{\partial \eta} \end{bmatrix} = \begin{bmatrix} \frac{\partial x}{\partial \xi} & \frac{\partial y}{\partial \xi} \\ \frac{\partial x}{\partial \eta} & \frac{\partial y}{\partial \eta} \end{bmatrix} \begin{bmatrix} \frac{\partial G_i}{\partial x} \\ \frac{\partial G_i}{\partial y} \end{bmatrix} = J \begin{bmatrix} \frac{\partial G_i}{\partial x} \\ \frac{\partial G_i}{\partial y} \end{bmatrix},$$

where J is the Jacobi matrix, which depends on the local coordinates. The differential element of area, according to [2], is

$$dxdy = |J| d\xi d\eta, \quad (13)$$

in which $|J|$ is the Jacobi determinant, or Jacobian of transformation.

By using (12) we find the global derivatives as

$$\begin{bmatrix} \frac{\partial G_i}{\partial x} \\ \frac{\partial G_i}{\partial y} \end{bmatrix} = J^{-1} \begin{bmatrix} \frac{\partial G_i}{\partial u_1} - \frac{\partial G_i}{\partial u_3} \\ \frac{\partial G_i}{\partial u_2} - \frac{\partial G_i}{\partial u_3} \end{bmatrix}.\quad (14)$$

Deriving J from the basis functions G_i , $i = 1, \dots, q$, which define the coordinate mapping (4), we obtain

$$J = \begin{bmatrix} \sum \frac{\partial G_i}{\partial \xi} p_i^x & \sum \frac{\partial G_i}{\partial \xi} p_i^y \\ \sum \frac{\partial G_i}{\partial \eta} p_i^x & \sum \frac{\partial G_i}{\partial \eta} p_i^y \end{bmatrix} = \begin{bmatrix} \frac{\partial G_1}{\partial u_1} - \frac{\partial G_1}{\partial u_3} & \frac{\partial G_2}{\partial u_1} - \frac{\partial G_2}{\partial u_3} & \dots \\ \frac{\partial G_1}{\partial u_2} - \frac{\partial G_1}{\partial u_3} & \frac{\partial G_2}{\partial u_2} - \frac{\partial G_2}{\partial u_3} & \dots \end{bmatrix} P. \quad (15)$$

Global matrices A , M and R are filled in by the local-to-global mapping. A concept of element matrices is fully described in [12]. The global matrix breaks up into sums of elemental contributions A^e , $e = 1, \dots, m$, where m is the number of elements.

Integration limits are changed to limits corresponding to a triangle. Finally, using formulas (13)-(15), the element stiffness and mass matrices are computed as follows

$$A^e = \int_0^1 \int_0^{1-\eta} \begin{bmatrix} \frac{\partial G^e}{\partial x} & \frac{\partial G^e}{\partial y} \end{bmatrix} \begin{bmatrix} \frac{\partial G^e}{\partial x_e} \\ \frac{\partial G^e}{\partial y} \end{bmatrix} |J| d\xi d\eta, \quad M^e = \int_0^1 \int_0^{1-\eta} (G^e)^T G^e |J| d\xi d\eta. \quad (16)$$

A transformed integral in the boundary matrix R should be computed along a curve, which represents the boundary $\partial\Omega^e$ of the triangular element Ω^e . According to the formula for computing curvilinear integrals, we write the element boundary matrix as

$$R^e = \int_0^1 \kappa (G^e)^T G^e \|(\partial\Omega^e)'_\sigma\| d\sigma. \quad (17)$$

4 Results

We solve the model problem (5) with Dirichlet boundary conditions (6). A few mode shapes are found on the circular domain Ω , which is constructed by using ERBS triangles, as shown in Figure 4. Approximations are found by formulas (9), (16)-(17) and compared with the exact solution (7).

The errors are presented in Figure 5 and computed as functions of the approximation for each of the considered mode. The error is approximated in L^2 -norm

$$\|\vartheta - \vartheta_h\| = \sqrt{\int_\Omega |\vartheta - \vartheta_h|^2 d\Omega}.$$

Figure 4 shows the construction of the circular domain formed by ERBS triangles and two types of local Bézier triangles: of degree 1 and 2, respectively. One of the resulting elements Ω^e is shown for both cases as a circle sector. Points on the element represent local parameters. One can see that on Figure 4(b) parameters are distributed more uniformly compared to Figure 4(a). By flexibility of ERBS triangle construction, we can construct specific parameter distribution, taking into account derivatives of the target surface.

Figure 6 demonstrates the results of the algorithm implementation. Simple shapes of the solution can be handled by the first degree of local triangles at the same accuracy level as for the second degree local triangles, for example for modes (0, 1), (0, 2), (2, 1). On the other hand, the appearance of the nodal circles together with nodal diameters immediately implies incrementation of the degree of local triangles. For example, the mode (1, 2) has some irregularities on the local degree $d = 1$, comparing with degree 2. It can be explained such as the shape of this mode is too complex for such low degree of local triangles.

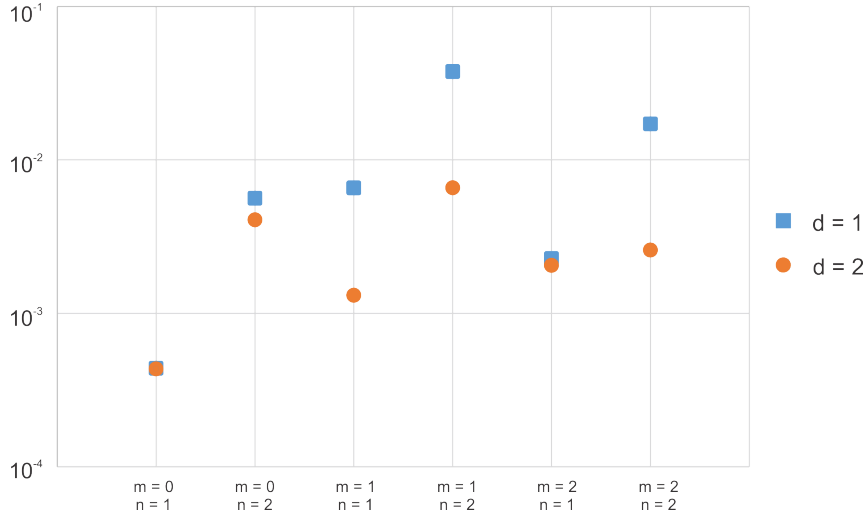


Figure 5: Comparison of L^2 -error for different mode-shapes and their FEM approximation by using two types of local triangles: of the first ($d = 1$) and second ($d = 2$) degree.

5 Conclusion

We have successfully implemented the finite element method that solve the eigenvalue problem on a circular membrane with fixed outer boundary, where elements are represented as ERBS triangles.

Increasing the degree of local triangles, one can provide many different approximations of the initial surface, which satisfy the required intrinsic properties of its geometry. Blending splines allow for accurately approximation of the boundary while keeping a coarse discretization of the domain. Even complex smooth domains can be constructed on a base of a few triangular elements. The overlapping of local triangles allows us to provide a flexible handling of the surface while preserving the smoothness of the initial domain, also over the nodes and edges.

The use of finite elements based on ERBS-triangles improves the computational efficiency. The structure of local triangles and a symmetric basis allow for the preliminary computation of integrals constituting the stiffness and mass matrices. Based on this, one can parallelize the computational process. Combining the above with the fact that the computations are performed on a very coarse mesh, we conclude that the proposed algorithm can be effectively optimized.

As future work we consider the development of automatic mesh generation, optimization of computations and a more thorough mathematical analysis of the presented basis functions.

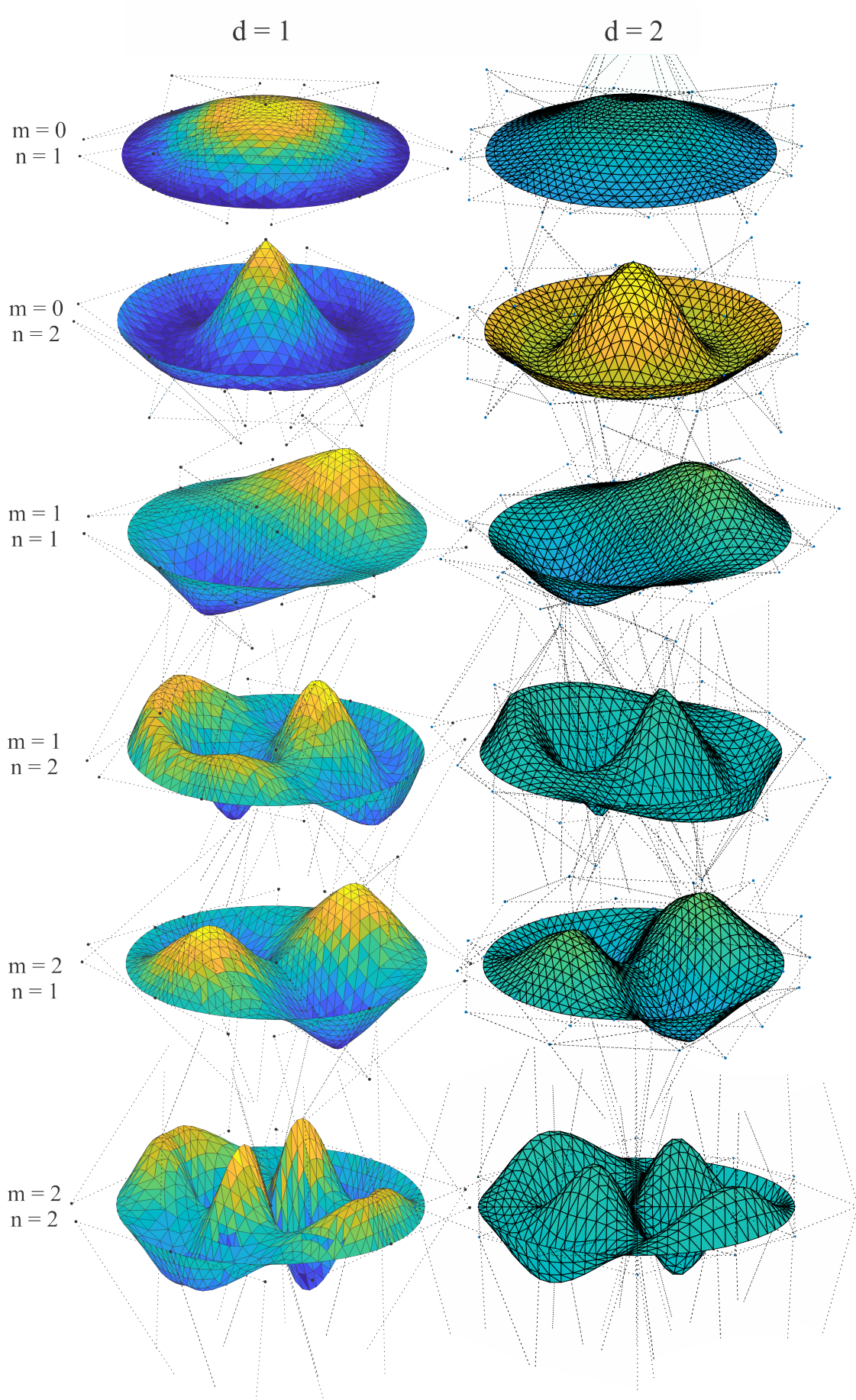


Figure 6: First few mode shapes, obtained by FEM utilizing ERBS triangles as elements. Two types of local triangles are presented: Bézier triangles of the first degree (left hand side), and of the second degree (right hand side). Local triangles are shown by points and dotted lines.

References

- [1] T.J.R. Hughes, J.A. Cottrell, and Y. Bazilevs. Isogeometric analysis: CAD, finite elements, NURBS, exact geometry and mesh refinement. *Computer Methods in Applied Mechanics and Engineering*, 194:4135–4195, 2005.
- [2] L. Meirovitch. *Principles and Techniques of Vibrations*. Prentice-Hall, Inc., Upper Saddle River, New Jersey, 1997.
- [3] L.T. Dechevsky, A. Lakså, and B. Bang. Expo-Rational B-Splines. *International Journal of Pure and Applied Mathematics*, 27(3):319–367, 2006.
- [4] A. Lakså. *Blending technics for curve and surface constructions*. Narvik University College, Narvik, Norway, 2006.
- [5] R. Dalmo, J. Bratlie, B. Bang, and A. Lakså. Smooth spline blending surface approximation over a triangulated irregular network. *International Journal of Applied Mathematics*, 27(1):109–119, 2014.
- [6] L.T. Dechevsky, P. Zanaty, A. Lakså, and B. Bang. First instances of generalized expo-rational finite elements on triangulations. *In: Applications of Mathematics and Engineering and Economics 2011*, 1410:49–61, 2011.
- [7] P. Zanaty. Finite element methods based on a generalized expo-rational B-splines with harmonic polynomial coefficients. *International Journal of Applied Mathematics*, 26(3):379–390, 2013.
- [8] M.-J. Lai and L.L. Schumaker. *Spline Functions on Triangulations*. Cambridge University Press, Cambridge, UK, 2007.
- [9] P. Hagedorn and A. DasGupta. *Vibrations and Waves in Continuous Mechanical Systems*. Wiley, 1st edition, 2007.
- [10] M.G. Larson and F. Bengzon. *The Finite Element Method: Theory, Implementation, and Practice*. Springer, 2010.
- [11] O.C. Zienkiewicz, R.L. Taylor, and J.Z. Zhu. *The Finite Element Method: Its Basis and Fundamentals*. Elsevier Butterworth-Heinemann Linacre House, Jordan Hill, Oxford, 6th edition, 2005.
- [12] T.J.R. Hughes. The Finite Element Method: Linear Static and Dynamic Finite Element Analysis. *Computer-aided civil and infrastructure engineering*, 4(3):245–246, 1989.